Dipolarization fronts and associated auroral activities: 2. Acceleration of ions and their subsequent behavior

X.-Z. Zhou,[1] Y. S. Ge,[2] V. Angelopoulos,[1] A. Runov,[1] J. Liang,[3] X. Xing,[4] J. Raeder,[2] and Q.-G. Zong[5]

[1] We present case studies of THEMIS multipoint observations of ion distributions in the magnetotail plasma sheet at various locations upstream of earthward-propagating dipolarization fronts. Observations made near the neutral sheet show a characteristic signature, enhancements of earthward-moving ion fluxes about 30 s before dipolarization front arrival. In previous studies, this signature has been well explained as front-reflected ions confined to a region characterized by their gyroradii over the background B_z field that coexist with the ambient population. However, at higher latitudes near the plasma sheet boundary layer, observations suggest that earthward-moving ions appear a few minutes earlier than at the central plasma sheet, indicating that the ions reflected at the same dipolarization front could access farther toward the Earth at higher latitudes. These observed phenomena, as also stated in our companion paper, are associated with transient intensifications of proton auroral brightness, which suggests a direct connection between magnetospheric and ionospheric signatures during geomagnetic disturbed conditions. We carry out numerical simulations and theoretical analysis of ion dynamics to interpret and reproduce these observations, to improve our understanding of interactions between earthward-propagating fronts and the ambient plasma in the near-Earth magnetotail, and to establish the proton auroral effects of dipolarization fronts.

Citation: Zhou, X.-Z., Y. S. Ge, V. Angelopoulos, A. Runov, J. Liang, X. Xing, J. Raeder, and Q.-G. Zong (2012), Dipolarization fronts and associated auroral activities: 2. Acceleration of ions and their subsequent behavior, *J. Geophys. Res.*, *117*, A10227, doi:10.1029/2012JA017677.

1. Introduction

[2] Dipolarization fronts (DFs), earthward-propagating structures with step-like enhancements of the northward magnetic field B_z in the magnetotail plasma sheet [e.g., *Nakamura et al.*, 2002; *Runov et al.*, 2009; *Sergeev et al.*, 2009; *Hwang et al.*, 2011], have often been observed near the leading edge of bursty bulk flows (BBFs) [*Angelopoulos et al.*, 1994]. Interpreted as vertical thin current sheets embedded within the horizontal tail current sheet, dipolarization fronts have been suggested to be boundaries separating hot, tenuous BBF plasma from the ambient colder, denser plasma sheet population [*Sergeev et al.*, 2009; *Runov et al.*, 2011a; *Zhang et al.*, 2011].

[3] According to superposed epoch analyses of Geotail [*Ohtani et al.*, 2004] and THEMIS [*Runov et al.*, 2011a] dipolarization front observations, sharp B_z enhancements are typically preceded by a minor B_z dip and succeeded by a gradual B_z reduction. These fronts have been traditionally interpreted either as BBF-type flux ropes [*Slavin et al.*, 2003] or as nightside flux transfer events (NFTEs) [*Sergeev et al.*, 1992]. Recently it has been suggested that DF signatures could be well reproduced by impulsive magnetic reconnection in kinetic simulations [*Sitnov et al.*, 2009]. After their generation, dipolarization fronts have been observed [*Runov et al.*, 2009, 2011b, 2012] and simulated [*Ge et al.*, 2011; *Birn et al.*, 2011] to propagate earthward coherently over a macroscopic distance of 10 R_E in a few minutes. Therefore, it is important to investigate the impact of these earthward-propagating structures on the near-Earth space.

[4] *Li et al.* [2011] proposed that a dipolarized flux tube could compress the ambient plasma, building up pressure gradient forces ahead of the front [*Xing et al.*, 2012] and establishing a plasma flow field surrounding the flux tube. Ambient plasma compression has been also recognized as the

---

[1]Department of Earth and Space Sciences and Institute of Geophysics and Planetary Physics, University of California, Los Angeles, California, USA.

[2]Space Science Center, University of New Hampshire, Durham, New Hampshire, USA.

[3]Department of Physics and Astronomy, University of Calgary, Calgary, Alberta, Canada.

[4]Department of Atmospheric and Oceanic Science, University of California, Los Angeles, California, USA.

[5]Institute of Space Physics and Applied Technology, Peking University, Beijing, China.

Corresponding author: X.-Z. Zhou, Department of Earth and Space Sciences, University of California, Los Angeles, CA 90095, USA. (xzhou@igpp.ucla.edu)

recoil force on DF-associated flow bursts that explains the observed overshoot and rebound of bursty bulk flows [*Panov et al.*, 2010].

[5] In the kinetic framework, the MHD picture of plasma compression could be understood as upstream ambient particles encountering the approaching front and being accelerated at it and reflected earthward [*Shabansky*, 1971; *Zhou et al.*, 2010; *Wu and Shay*, 2012]. The accelerated and reflected ions could be observed in the upstream central plasma sheet (CPS) as an additional population with earthward velocities superimposed over the ambient plasma. These ions, however, are not expected to appear beyond their gyroradii over background B_z in the upstream CPS. Statistical studies of THEMIS observations have further suggested that the size of the reflected ion accessibility region (their gyroradii over background B_z) would determine the duration of earthward precursor flows ahead of the front [*Zhou et al.*, 2011], typically a few tens of seconds [*Runov et al.*, 2011a].

[6] It should be noted that the aforementioned studies focus only on observations in the CPS, not those farther away from the neutral sheet. In this paper, we examine various ion distribution patterns at different locations upstream of earthward-propagating dipolarization fronts using THEMIS multipoint observations [*Angelopoulos*, 2008] of two DF events in March 2009. The standard picture, i.e., the appearance of an earthward-moving ion population superimposed on ambient plasma ∼30 s before DF arrival, was observed at the CPS in both events. THEMIS probes located at higher latitudes near the plasma sheet boundary layer (PSBL), on the other hand, consistently observed accelerated earthward-moving ions a few minutes earlier.

[7] Given the dominance of the magnetic field B_x component near the PSBL, the presence of accelerated ions moving earthward upstream of the front suggests that many of these ions could stream along field lines and eventually precipitate in the ionosphere, resulting in transient intensifications of proton auroral brightness. These auroral observations, in conjunction with THEMIS measurements, are also shown in this paper, and in more detail in the companion paper [*Ge et al.*, 2012].

[8] After presenting the observations, we follow the same simulation approach used in *Zhou et al.* [2011] to reproduce the observed ion distribution patterns at different locations. The theory of ion dynamics and trajectories in the thin current sheet [*Büchner and Zelenyi*, 1989] is then applied to explain the global patterns of ion distribution functions upstream of the front. By making these efforts, we seek to improve our knowledge of interactions between dipolarization fronts and the ambient plasma in the near-Earth magnetotail, and to establish the connection between dipolarization fronts and proton auroral signatures in the ionosphere.

2. Instrumentation

[9] This study uses data from the following THEMIS instruments: (1) the fluxgate magnetometer (FGM) [*Auster et al.*, 2008], which provides DC magnetic field measurements; (2) the electrostatic analyzer (ESA) [*McFadden et al.*, 2008], which provides particle distribution functions in the 5 eV to 25 keV energy range; and (3) the solid state telescope (SST) [*Angelopoulos*, 2008], which detects high-energy (25 keV to 1 MeV) particle distributions.

[10] During one of the events studied (19 March 2009 event), three THEMIS probes (P1, P2 and P3) were located in the Earth's shadow with no sun-pulse signal input to keep track of probe spin behavior. Additional calibration procedures had been carried out before these observational data were used.

[11] This study also uses the optical data of 486-nm H-β line emissions to present proton auroral intensities. These data are available via the NORSTAR Meridian Scanning Photometer (MSP) at Fort Smith (FSMI), which sweeps through the meridian sky at two scans per minute.
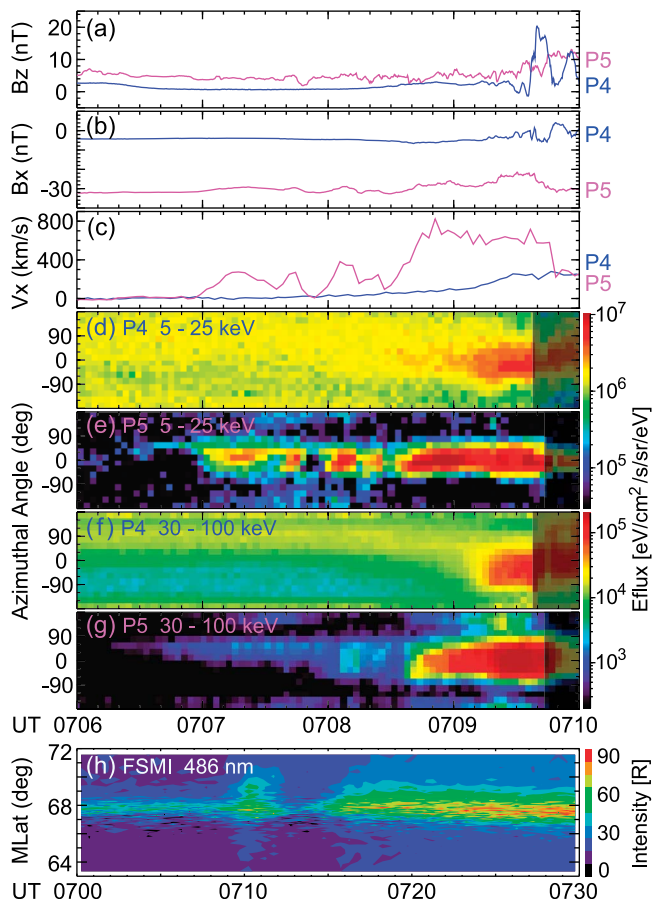
3. The 18 March 2009 Event

[12] Figures 1a–1g provide a 4 min overview of THEMIS P4 and P5 observations during the 18 March 2009 dipolarization front event. Both probes were located in the near-Earth magnetotail: at 0710 UT, P4 was at GSM coordinates [−11.4, 1.0, −1.6] R_E, and P5 was ∼1 R_E southward at [−11.3, 0.9, −2.6] R_E. This was by design of the THEMIS 2009 tail season, to have P5 staying 1 R_E southward of P4 so as to observe vertical gradients [*Sibeck and Angelopoulos*, 2008].

[13] The observed time series of magnetic B_x components shows that P4 remained at the central plasma sheet (with $B_x \sim -5$ nT), and P5 was located near the plasma sheet boundary layer ($B_x \sim -30$ nT, plasma $\beta \sim 0.1$). Both probes experienced negligible magnetic fluctuations until a sharp B_z enhancement of ∼20 nT was observed at P4 at 07:09:36 UT indicating the arrival of a dipolarization front. The B_z enhancement at P5, although less significant in amplitude (∼5 nT), was still conspicuous at 0709:42 UT.

[14] Figures 1d–1g show P4 and P5 observations of ion differential energy fluxes as functions of equatorial azimuthal angle and time at two different energy ranges. At 0709 UT, over 30 s before dipolarization front arrival, P4 observed gradual enhancements of ion fluxes at both 5–25 and 30–100 keV energy ranges in the earthward direction (with a minor component in the dawnward direction), which resulted in an increased earthward flow velocity. These signatures are expected in the central plasma sheet upstream of earthward-propagating fronts [*Zhou et al.*, 2011], where ions previously accelerated by and reflected at the front coexist with the ambient population in a confined region characterized by their gyroradii over background B_z field. According to *Zhou et al.* [2011], the approximately 30-sec duration of precursor flows ahead of the front corresponds to the size of the DF-reflected ion accessibility region.

[15] The earthward precursor flows also appeared at P5 near the PSBL, with the velocity V_x rising to 800 km/s. In fact, the earthward-moving ions started to appear at P5 by 0707 UT, 2 min earlier than at P4, and the ion fluxes remained peaked in the earthward direction until after front arrival. In other words, the accessibility limit of the DF-reflected ions in the upstream CPS does not apply here at higher latitudes, with the appearance and dominance of DF-reflected ions in an extended region far beyond the limit. Given that the magnetic field was predominantly in the $-x$ direction near the PSBL, these earthward-moving ions are mostly anti-parallel to the field lines (for ion pitch angle

Figure 1. Overview of the 18 March 2009 dipolarization front event. THEMIS P4 and P5 observations of GSM magnetic (a) B_z and (b) B_x components; (c) plasma flow velocity in the GSM x direction. (d) THEMIS P4 and (e) P5 observations of ion differential energy fluxes versus equatorial azimuthal angle in the probe spin plane, in the 5–25 keV energy range. Here $0°$ and $90°$ correspond to the earthward and duskward fluxes, respectively. The shaded regions suggest time intervals after front arrival at the corresponding probe. (f and g) Same format as Figures 1d and 1e, but displaying the ion spectra in the 30–100 keV energy range. (h) Fort Smith MSP observations of the 486 nm proton auroral emission.

distributions, see Figure 6h of the *Ge et al.* [2012] companion paper).

[16] The ionospheric counterpart of these observations, observed by the Fort Smith MSP scanning in the same meridian as P5 at this time, is shown in Figure 1h. The H-β keogram clearly shows a transient (~2 min) intensification and poleward expansion of the proton auroral brightness at ~0710 UT in association with the dipolarization front. The enhanced ion precipitations, observed in a latitude-elongated region, are expected to result from the dominance of DF-reflected ions moving along magnetic field lines in an extended region upstream of the front. Further details of these observations are given in the *Ge et al.* [2012] companion paper.

[17] Note that the ion distribution signatures observed in the 18 March 2009 event were not unique: we have surveyed

the THEMIS data and found many events with very similar features, although THEMIS is not necessarily conjugate to the ground-based MSPs in most of the cases. Among these events is the dipolarization front that appeared on the following day (see next section).

4. The 19 March 2009 Event

[18] The 19 March 2009 event is one of the six selected cases shown in *Runov et al.* [2011a] with multiple probes observing the same dipolarization front from different locations. The configuration of the five THEMIS probes in the GSM xz and xy planes at 0825 UT is shown in Figures 2a and 2b. These probes were clustered in the near-Earth magnetotail with x between -11 R_E and -14 R_E. The exact GSM positions of P1, P2, P3, P4 and P5, at 0825 UT, were [-12.3, 0.7, 0.0], [-13.4, 0.7, -0.6], [-11.4, -0.4, -0.9], [-11.5, 0.6, -1.1] and [-11.5, 0.7, -2.1] R_E, respectively.

[19] Figure 2c shows the time series of the observed B_z field at all five probes during a 4-min interval. The dipolarization front, identified by sharp B_z enhancements, was detected by P2, P1, P4 and P3 consecutively between 0825 and 0826 UT. The propagating velocity of the front, according to the estimation of *Runov et al.* [2011a] by using the time delays between front arrivals at different probes, is ~550 km/s in the earthward direction. The presence of sharp B_z enhancements on all four probes also suggest that the front has a width in y of greater than 1 R_E. On the other hand, the B_z variations were much more gradual at P5, which was located 1 R_E south of P4 near the PSBL (plasma $\beta \sim 0.3$ at 0824 UT).

[20] Figures 2d–2h show the THEMIS five-spacecraft observations of azimuthal ion spectra in the 5–25 keV energy range. Once again the expected upstream signatures described in *Zhou et al.* [2011] were well observed by P2, P1, P4 and P3 in the CPS: an ion population moving earthward (and slightly dawnward) superimposed on ambient plasma ~30 sec before front arrival. Even though P5 did not observe the sharp B_z enhancement at higher latitudes, the fluxes of earthward-moving ions started to gradually increase by 0823 UT, about 2 min earlier than at P4. These characteristic signatures are also presented in the SST energy range of 30–100 keV, shown in Figures 2i and 2j.

[21] These observations, together with those of the previous event, suggest that earthward-moving ions reflected by the same dipolarization front could access a much more extended region ahead of the front near the PSBL than near the neutral sheet. In the next sections, we follow the same backward-tracing Liouville approach as described in *Zhou et al.* [2011] to simulate and reproduce key signatures of ion distributions observed during these events, and to quantify the flux levels of DF-reflected keV ions that can be associated with proton aurora.

5. Simulations

[22] The simulation approach is based on Liouville's theorem [*Birn and Hesse*, 1994; *Schwartz et al.*, 1998; *Zhou et al.*, 2009]. Given the initial condition of location-dependent ion distribution functions $f(\mathbf{r}_0, \mathbf{v}_0, t_0)$ in the equilibrium tail plasma sheet with no impact from the dipolarization front, the approach takes advantage of test-particle simulations to determine ion distributions $f(\mathbf{r}, \mathbf{v}, t)$ as functions of
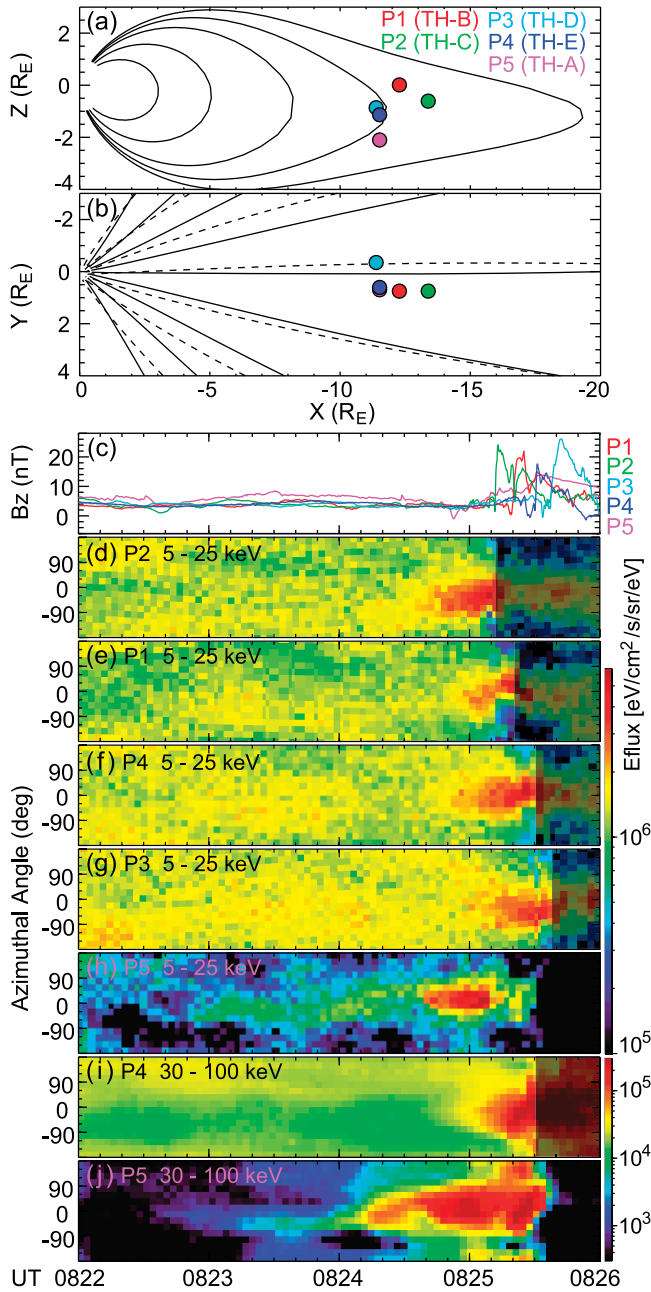
Figure 2. Overview of THEMIS five-point observations during the 19 March 2009 event. THEMIS probe positions at 0825 UT, in the GSM (a) xz and (b) xy planes, superposed over magnetic field lines from the T96 model [*Tsyganenko*, 1995]. (c) Time series of GSM B_z at five probes. Differential energy fluxes of (d–h) 5–25 keV ions at five THEMIS probes, and of (i and j) 30–100 keV ions at P4 and P5, versus azimuthal angle in the same format as in Figures 1d–1g. Note that the spectra have been recalibrated to ensure that the 0° and 90° angles correspond to the earthward and duskward directions, respectively.

distribution functions cannot be used to provide feedback to the field evolutions, the simple approach has the advantage that one can easily adjust the model to isolate different processes and better reveal the underlying physics. As the first step, here we use the generalized *Harris* [1962] model, which has been described and applied in *Zhou et al.* [2011], as the initial condition of the simulation runs. The model, an equilibrium solution of the Maxwell-Vlasov equations for a two dimensional plasma sheet, self-consistently provides the magnetic field (B_x and B_z components) and particle distribution functions everywhere within the equilibrium.

[24] To match the THEMIS five-spacecraft observations of the quasi-steady plasma sheet during the 19 March 2009 event well before dipolarization front arrives, the initial equilibrium plasma sheet is centered at $z_0 = -0.5\ R_E$, and the following parameters are selected: B_n, the magnetic field B_z at the center of the plasma sheet, equals 3 nT; V_T, the thermal ion velocity within the entire plasma sheet, is 850 km/s; n_0, the plasma density at $(-10, -0.5)\ R_E$, is 0.6 cm^{-3}; L, the plasma sheet half-thickness at $x = -10\ R_E$, is 1 R_E; B_0, the lobe magnetic field at $x = -10\ R_E$, is 45 nT. The configuration of the modeled plasma sheet is given in Figure 3a, which shows spatial distributions of plasma density as well as magnetic field lines. The positions of the five THEMIS probes within the initial equilibrium are also indicated.

[25] In addition to the initial condition, the Liouville simulation also requires that the magnetic and electric fields be prescribed as the front propagates earthward so the ion trajectories can be calculated. Here we assume that the magnetic and electric fields are the same as the fields in the initial equilibrium, except for the superposition of
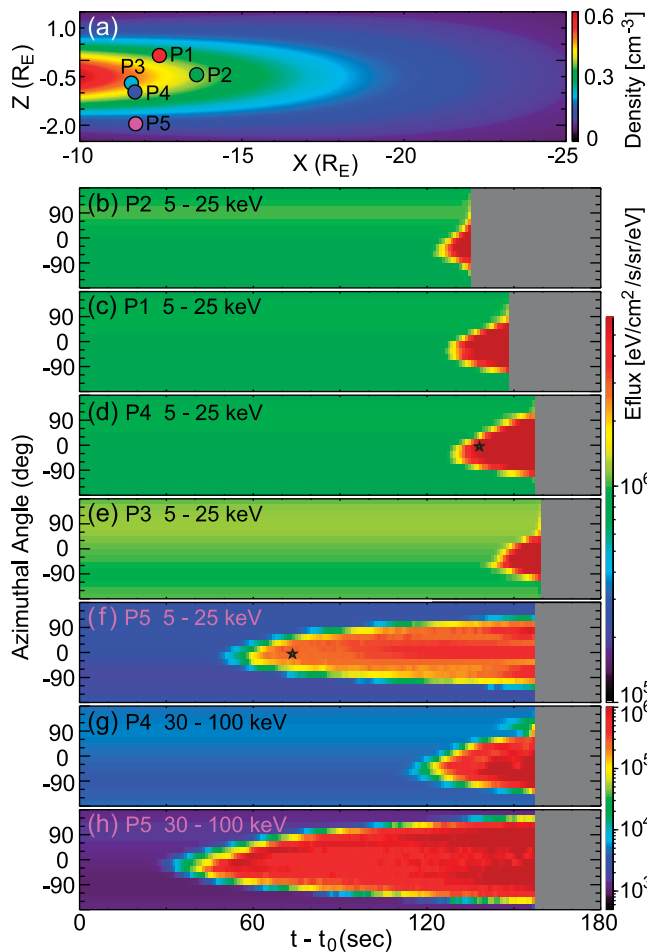
$$B_{zf}(x,t) = \frac{B_f}{2}\left\{1 - \tanh\left[\frac{x - x_{f0} - V_f(t - t_0)}{L_f}\right]\right\}, \quad (1)$$

$$E_{yf}(x,t) = V_f B_{zf}(x,t), \quad (2)$$

to model the earthward propagation of a hyperbolic-tangent front at the speed of $V_f = 550$ km/s. Here $B_f = 20$ nT is the B_z enhancement associated with the front; $L_f = 0.1\ R_E$ is the characteristic DF half-thickness; and $x_{f0} = -25\ R_E$ is the initial DF location at $t = t_0$. The assumption ensures that the magnetic field remains divergence-free, and the electric field is always perpendicular to the magnetic field. Also note that the modeled electric field is built up in accordance with Faraday's law, which would become negligible in the rest frame of the front (given $B_f \gg B_n$ in this case).

[26] The simulation, which stops as the front arrives at each probe to avoid taking into account the different plasma population of BBFs behind the front, results in the ion azimuthal angular spectra (in the energy ranges of 5–25 keV and 30–100 keV) shown in Figures 3b–3h. The key features observed by THEMIS probes (shown in Figure 2) are well reproduced by the simulation: the earthward-moving ion fluxes enhance first at the probe farthest from the neutral sheet (near the boundary layer), and then near the neutral sheet about 90 s later, still 20–30 seconds prior to the front arrival.

[27] Differences in appearance time of earthward-moving ions at different locations are expected to be caused by the distinct trajectories along which these ions would follow in

time and location, by tracing the ion trajectories backward in time to identify their initial locations $\mathbf{r}_0$ and velocities $\mathbf{v}_0$ at t_0, with $f(\mathbf{r}, \mathbf{v}, t) = f(\mathbf{r}_0, \mathbf{v}_0, t_0)$.

[23] Despite the limitations of the test-particle simulations on self-consistency, especially in that the computed particle

Figure 3. Simulation results of the 19 March 2009 event. (a) The initial condition: plasma density distributions in the equilibrium plasma sheet, with isodensity lines also delineating magnetic field lines; The simulated ion fluxes in the (b–f) 5–25 keV and in the (g and h) 30–100 keV energy range at the locations of THEMIS probes, in the same format as in Figures 2d–2j. The time intervals after front arrival, which run beyond the scope of this simulation, are shown as the shaded regions.

the upstream plasma sheet after being reflected by the front. Figure 4 shows two examples of ion trajectories obtained in the simulation. These ions are selected to have the same velocity (1380 km/s earthward and 20 km/s dawnward, denoted as the black stars in Figures 3d and 3f) when one of them (ion A) reaches P4 at $t = t_0 + 138$ s and the other (ion B) reaches P5 at $t = t_0 + 73$ s. Obviously both ions belong to the superimposed earthward-moving population that appears well ahead of the front, but they are otherwise not special.

[28] The trajectory of ion A, which eventually reaches P4 in the central plasma sheet, is shown in Figure 4a. The ion remains in the unperturbed plasma sheet upstream of the front with constant energy, until $t = t_0 + 123$ s when it encounters the approaching front and starts to gyrate around the enhanced B_z field in the duskward direction. The gyrating motion lasts a few seconds, during which the ion finishes a half-gyro cycle, and the ion kinetic energy increases by

~5 keV due to the presence of the DF-associated dawn-dusk electric field (2). The accelerated ion is then reflected back to the region ahead of the front, before being captured by P4 in approximately 10 s.

[29] As expected, the ion trajectory is very similar to the sample ion trajectory shown in *Zhou et al.* [2011] (see their Figure 3). Also note that the DF-reflected ion, even if not captured by P4, would not go much farther earthward within the CPS, as evidenced by the absence of ion flux enhancements 10 s earlier at $t = t_0 + 128$ s (see the simulation results shown in Figure 3d). As discussed in *Zhou et al.* [2011], the ion accessibility limit within the CPS is caused by the finite B_z field (and therefore the finite ion gyroradius over B_z) ahead of the front.

[30] Figure 4b suggests the trajectory of ion B, which eventually reaches P5 at higher latitudes. The ion encounters the front at $t = t_0 + 14$ s, and then returns to the upstream region a few seconds later with energy enhancements of about 5 keV. In the next 55 s, the ion keeps moving earthward regardless of the nominal accessibility limit, until being captured by P5 at higher latitudes 7 R_E ahead of the front.

[31] A straight-forward explanation for the invalidation of the nominal ion accessibility limit near the PSBL is the dominance of B_x over B_z; the earthward moving ions would likely stream along field lines rather than gyrating around B_z in the xy plane. Detailed interpretations of these results, however, require the systematic theory of ion motion in the unperturbed current sheet [*Büchner and Zelenyi*, 1989].
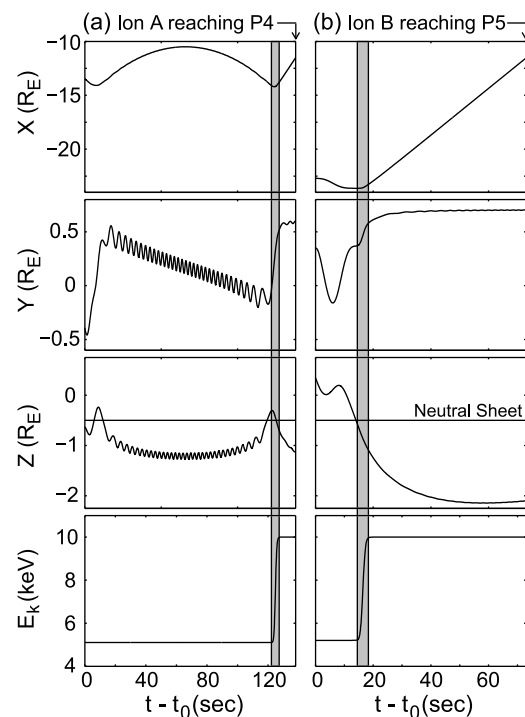
Figure 4. Typical ion trajectories in the simulation run. (a) Ion A, which reaches P4 at $t = t_0 + 138$ s, and (b) ion B, which reaches P5 at $t = t_0 + 73$ s. (top to bottom) The x, y, z positions and the kinetic energy of the ions as functions of time. The shaded areas suggest time intervals when the ion stays at or behind the front experiencing enhanced B_z and E_y fields.
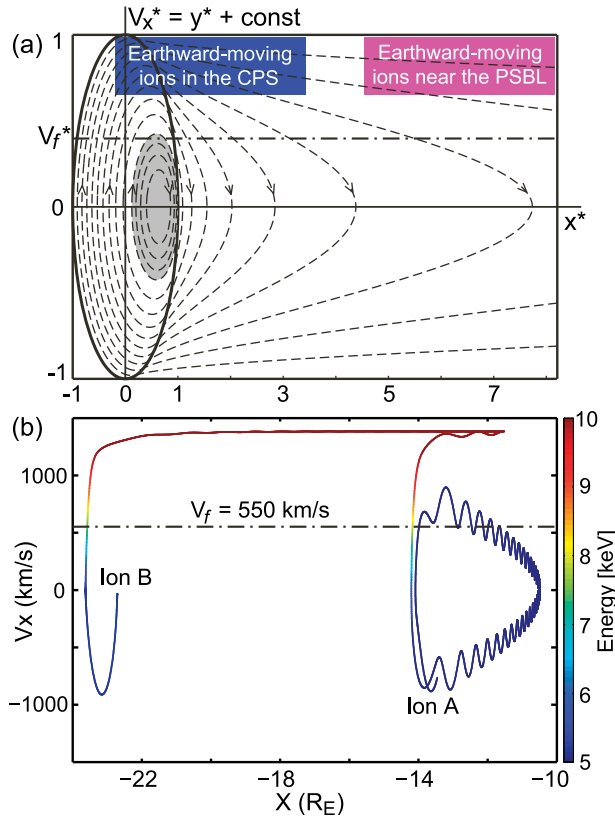
Figure 5. The x versus V_x phase diagram of ion motion in the magnetotail plasma sheet. (a) Replotted from Figure 9 of *Büchner and Zelenyi* [1989], theoretical diagram of ion slow xy-motion in the unperturbed current sheet, with fast z-oscillations decoupled. The solid ellipse ($x^{*2} + V_x^{*2} = 1$) separates meandering (inside the ellipse) and noncrossing regimes of particle z oscillations. (b) The x versus V_x diagram of two typical ions (trajectories shown in Figure 4) from the simulation run, with line colors suggesting ion kinetic energy. The fast z oscillations are not decoupled here, which results in wave-like fluctuations superposed over the slow motion.

In the next section, that theory is briefly reviewed and then applied to the ion trajectories in the quasi-steady upstream region after their reflection, so that one can better understand the observed and simulated ion distribution patterns at different locations ahead of the front.

6. Interpretations

[32] The theory of *Büchner and Zelenyi* [1989] deals with particle trajectories in the magnetotail where the minimum radius of curvature of magnetic field lines R_c is smaller than the neutral sheet ion gyroradius R_L. In the equilibrium plasma sheet model adopted here, R_c equals $0.067 R_E$ at $x = -10 R_E$, and the gyroradius of a 10 keV proton is $0.76 R_E$, which well satisfies the $R_c < R_L$ condition and therefore invalidates the conventional guiding center approximation as well as traditional adiabatic invariants. The theory, developed based on pioneering works [e.g., *Speiser*, 1965; *Sonnerup*, 1971; *Chen and Palmadesso*, 1986] on particle dynamics in the current sheet, suggests that particle trajectories are characterized by the superposition of fast oscillations in the z direction and slow motion mostly in the xy plane.

[33] On a fast z-oscillating timescale, an ion could either meander across or avoid the neutral sheet. These two different regimes of fast motion could be converted into each other during the slower xy-motion of the particle. The slow xy-motion, with fast oscillations decoupled, is visualized as dashed lines in Figure 5a by means of a $\{x, V_x\}$ phase diagram. Here V_x is normalized by the ion total velocity V_t, and x is normalized by the characteristic ion gyroradius $\rho = m_i V_t / e B_n$. The vertical axis ($V_x^* = V_x / V_t$) could be treated as $y^* = y/\rho$ as well, if B_n, the magnetic field B_z component, is constant within the entire current sheet.

[34] According to *Büchner and Zelenyi* [1989], ions located inside the solid ellipse ($x^{*2} + V_x^{*2} = 1$) would meander across the neutral sheet within the fast-motion timescale; those to the right would oscillate in the noncrossing regime. Therefore, ions in the shaded area of Figure 5a would remain in the meandering regime during their entire slow-motion cycle. This kind of ion trajectories, characterized by slow circular xy-motions and fast z-oscillations periodically traversing the neutral sheet, was named by *Büchner and Zelenyi* [1989] the ring-type trajectories.

[35] On the other hand, it could be seen that ions outside the shaded area would traverse the elliptical separatrix twice within each slow-motion cycle. In other words, ions initially meandering across the neutral sheet could be ejected into either hemisphere with positive V_x at the separatrix. These ions would move toward higher latitudes with decreasing velocities in the earthward direction, until reaching the turning point with greatest x and $|z - z_0|$ values. After that, they would be mirrored back and eventually return to the meandering regime inside the ellipse. *Büchner and Zelenyi* [1989] called this the cucumber-type trajectory.

[36] One of the inherent properties of the ion motion diagram shown in Figure 5a is that ions on the right side of the diagram (with significant x values) would have great $|z - z_0|$ values (the distances to the neutral sheet) as well [see *Zelenyi et al.*, 2011, Figure 5]. Therefore, the earthward-moving ions observed near the neutral sheet and near the PSBL would appear in the diagram's top left and top right corners (the blue and the magenta regions in Figure 5a), respectively.

[37] With the pictures of ion motion in the unperturbed current sheet in mind, we consider the effect of an earthward-propagating dipolarization front as the source of accelerated ions reflected and injected into the upstream current sheet (where the *Büchner and Zelenyi* [1989] theory applies). By definition, these ions should have greater V_x than the front propagating speed V_f when they depart from the dipolarization front. In other words, the new population of accelerated and reflected ions would appear in Figure 5a at the phase space above the dash-dotted line $V_x = V_f$, and they start to follow the dashed lines in the upstream region of the front.

[38] These ions, after reflected from the front and injected into the upstream current sheet, could not have traveled a large distance in x before entering the blue region, which agrees with the limited accessibility region ahead of the front in the central plasma sheet. These ions could remain in the CPS only if they turn dawnward and quickly decelerate in V_x (following the dashed lines pointing toward negative V_x and negative y), which could explain the CPS observations (see Figures 2d–2g, or see Figure 4d of *Zhou et al.* [2011]) and
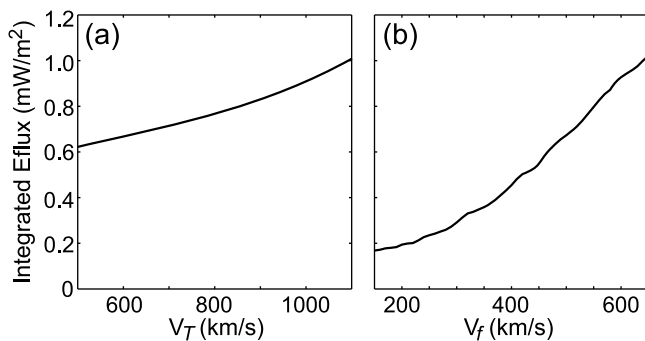
Figure 6. The simulation results of integrated energy fluxes of precipitating ions, as functions of (a) ion thermal velocity V_T in the unperturbed plasma sheet, with a fixed DF propagating speed of $V_f = 550$ km/s, and (b) DF propagating speed V_f, with a fixed V_T of 850 km/s. All the other parameters ($n_0 = 0.6$ cm^{-3}, $B_n = 3$ nT, $L = 1$ R_E, $B_0 = 45$ nT, $B_f = 20$ nT, and $L_f = 0.1$ R_E) are the same as those described in section 5.

simulations (Figures 3b–3e) that initial enhancements of ion fluxes near the neutral sheet ahead of the front are typically in the dawnward direction. On the other hand, ions with most significant V_x^* values in the blue region would follow the uppermost dashed lines and continue moving in the earthward direction, albeit at higher latitudes, and eventually reach the magenta region.

[39] The theoretical explanations could be compared directly with the ion trajectory samples shown in Figure 4, which are also presented here in the format of x versus V_x diagram in Figure 5b. The colored lines represent the ion kinetic energy along their trajectories: the portions with varying colors correspond to intervals when the ions are located at or behind the front experiencing enhanced B_z and E_y fields; those with constant colors (either blue or red) correspond to intervals when the ions stay in the upstream unperturbed plasma sheet where the *Büchner and Zelenyi* [1989] theory applies. It can be seen that the trajectories of ions A and B end at the same GSM x locations with the same V_x. However, as discussed previously, these two end points have different z values, and therefore correspond to the blue and the magenta regions in Figure 5a, respectively.

[40] Comparisons between Figures 5a and 5b clearly show that ion A initially follows a cucumber-type trajectory with constant energy in the upstream plasma sheet between $x = -14$ and $x = -10$ R_E. After encountering the front, the ion is quickly energized until its kinetic energy reaches 10 keV as it returns to the upstream region. During this interval, its V_x value changes from ~ -100 km/s to ~ 1200 km/s. Given the DF propagating speed V_f of 550 km/s, the ion reflection is found to be approximately elastic in the rest frame of the front, with approximately the same $|V_x - V_f|$ (~ 650 km/s) before and after the ion's DF-encounter due to the negligible electric field in the DF rest frame. After being reflected back to the upstream plasma sheet, the ion soon enters the blue region of Figure 5a, with V_x significantly greater than V_f, and is captured by P4 in approximately 10 sec.

[41] Ion B also experiences elastic reflection after encountering the front, and it again appears well above the $V_x = V_f$ line

in the blue region when it returns to the upstream region. The dominance of V_x (~ 1300 km/s) over other velocity components (given the total speed V_t of 1380 km/s) suggests a V_x^* value of nearly unity, and the ion would therefore follow the uppermost dashed lines of Figure 5a toward the magenta region. This is indeed the case, as we can see in Figure 5b that the ion continues moving in the earthward direction until captured by P5. In fact, V_x-dominated ions could stream almost unrestrictedly along field lines toward the Earth, eventually producing proton auroral intensifications in the ionosphere.

7. Discussions

[42] Our model allows us to estimate the integrated energy fluxes of precipitating ions associated with earthward-propagating dipolarization fronts. After reflection, an ion must appear at the very top portion of Figure 5a with V_x significantly greater than V_y and V_z components so that it can travel all the way to the Earth and precipitate in the ionosphere. Here we carry out the simulation using the same parameters adopted in section 5 and integrate the simulated earthward ion differential energy fluxes over energy, in the range of 1 keV and above to contribute to the proton aurora production [e.g., *Lummerzheim and Galand*, 2001]. The resulting integrated energy fluxes are calculated to be approximately 0.8 mW/m^2 ahead of front arrivals.

[43] According to the simulation, the integrated energy fluxes of precipitating ions are linearly correlated with the neutral sheet plasma density n_0 in the upstream equilibrium (not shown). Given a fixed n_0 of 0.6 cm^{-3}, the simulated energy fluxes also depend significantly on the ion thermal velocity V_T in the unperturbed plasma sheet and on the DF propagating speed V_f, as shown in Figure 6.

[44] It can be seen in Figure 6 that earthward-propagating fronts can produce precipitating ions with the typical integrated energy fluxes of 0.2–1 mW/m^2. The simulated ion precipitation becomes stronger with increasing speed of earthward-propagating DFs and with warmer ions in the unperturbed plasma sheet before front arrival. These values could be compared with the ionospheric observations of proton auroral intensities (see the companion paper by *Ge et al.* [2012]). Therefore, proton auroral imaging in the ionosphere, provided at high enough temporal resolution, may have the capability of tracing dipolarization front evolutions in the magnetotail plasma sheet.

8. Summary

[45] An interesting feature observed prior to arrival of earthward-propagating dipolarization fronts is enhancement of ion fluxes in the earthward direction, which leads to the appearance of precursor earthward plasma flows. In the study of these precursor flows, *Zhou et al.* [2010, 2011] have found them to be caused by the emergence of earthward-moving ions that have been accelerated by and reflected at the approaching front.

[46] It has been suggested that the DF-reflected ion population could only access a restricted region ahead of the front in the central plasma sheet. This scenario agrees with observed precursor flow durations (typically ~ 30 sec). Farther away from the neutral sheet, near the plasma sheet boundary layer,

however, DF-reflected ions are observed to appear even earlier (by a few minutes), which suggests an x-extended region with enhanced ion fluxes in the earthward direction. Ground-based photometers have observed the ionospheric counterpart of these observations, transient intensifications of proton auroral brightness in a latitude-elongated region.

[47] Test-particle simulations using Liouville's theorem reproduce the aforementioned ion distribution patterns observed at different locations. These signatures can also be understood in the context of the *Büchner and Zelenyi* [1989] theory of ion behavior in the plasma sheet, with the earthward-propagating front acting as the source of accelerated ions (with low $-V_x$ cutoffs) injected into the upstream plasma sheet. We further propose that these DF-reflected ions near the PSBL, as they are energized to several or a few tens of keV, can stream along magnetic field lines and eventually generate proton aurora, a direct consequence of magnetotail activities in the ionosphere.

[48] It should be pointed out that the presence of earthward-moving ions in the plasma sheet boundary layer is a frequently observed phenomenon not necessarily associated with dipolarization fronts [e.g., *Decoster and Frank*, 1979; *Eastman et al.*, 1984; *Grigorenko et al.*, 2009]. The typical crescent-shaped appearance of these ions in the velocity space [*Decoster and Frank*, 1979; *Angelopoulos et al.*, 1989] has been suggested to result from ion acceleration processes in the central plasma sheet, either caused by magnetic reconnection [*Onsager et al.*, 1991; *Hoshino et al.*, 1998] or by nonadiabatic particle orbits [*Ashour-Abdalla et al.*, 1993; *Grigorenko et al.*, 2009]. The ion DF-reflection process discussed in our study could be just another mechanism that contributes to the appearance of earthward-moving ions in the plasma sheet boundary layer, especially in the presence of earthward-propagating dipolarization fronts. We made no attempt here to exclude possibilities that other processes also play a role, as discussions of this topic are beyond the scope of this paper. More systematic investigations and further discussions are to be made in a separate study [*Zhou et al.*, 2012].

[50] Masaki Fujimoto thanks Christopher Cully and another reviewer for their assistance in evaluating this paper.

References

Angelopoulos, V. (2008), The THEMIS mission, *Space Sci. Rev.*, *141*, 5–34, doi:10.1007/s11214-008-9336-1.

Angelopoulos, V., R. C. Elphic, P. S. Gary, and C. Y. Huang (1989), Electromagnetic instabilities in the plasma sheet boundary layer, *J. Geophys. Res.*, *94*, 15,373–15,383, doi:10.1029/JA094iA11p15373.

Angelopoulos, V., C. F. Kennel, F. V. Coroniti, R. Pellat, M. G. Kivelson, R. J. Walker, C. T. Russell, W. Baumjohann, W. C. Feldman, and J. T. Gosling (1994), Statistical characteristics of bursty bulk flow events, *J. Geophys. Res.*, *99*, 21,257–21,280, doi:10.1029/94JA01263.

Ashour-Abdalla, M., J. P. Berchem, J. Buechner, and L. M. Zelenyi (1993), Shaping of the magnetotail from the mantle: Global and local structuring, *J. Geophys. Res.*, *98*, 5651–5676, doi:10.1029/92JA01662.

Auster, H. U., et al. (2008), The THEMIS Fluxgate Magnetometer, *Space Sci. Rev.*, *141*, 235–264, doi:10.1007/s11214-008-9365-9.

Birn, J., and M. Hesse (1994), Particle acceleration in the dynamic magnetotail: Orbits in self-consistent three-dimensional MHD fields, *J. Geophys. Res.*, *99*, 109–119, doi:10.1029/93JA02284.

Birn, J., R. Nakamura, E. V. Panov, and M. Hesse (2011), Bursty bulk flows and dipolarization in MHD simulations of magnetotail reconnection, *J. Geophys. Res.*, *116*, A01210, doi:10.1029/2010JA016083.

Büchner, J., and L. M. Zelenyi (1989), Regular and chaotic charged particle motion in magnetotaillike field reversals: 1. Basic theory of trapped motion, *J. Geophys. Res.*, *94*, 11,821–11,842.

Chen, J., and P. J. Palmadesso (1986), Chaos and nonlinear dynamics of single-particle orbits in a magnetotaillike magnetic field, *J. Geophys. Res.*, *91*, 1499–1508.

Decoster, R. J., and L. A. Frank (1979), Observations pertaining to the dynamics of the plasma sheet, *J. Geophys. Res.*, *84*, 5099–5121, doi:10.1029/JA084iA09p05099.

Eastman, T. E., L. A. Frank, W. K. Peterson, and W. Lennartsson (1984), The plasma sheet boundary layer, *J. Geophys. Res.*, *89*, 1553–1572.

Ge, Y. S., J. Raeder, V. Angelopoulos, M. L. Gilson, and A. Runov (2011), Interaction of dipolarization fronts within multiple bursty bulk flows in global MHD simulations of a substorm on 27 February 2009, *J. Geophys. Res.*, *116*, A00I23, doi:10.1029/2010JA015758.

Ge, Y. S., X.-Z. Zhou, J. Liang, J. Raeder, M. L. Gilson, E. F. Donovan, V. Angelopoulos, and A. Runov (2012), Dipolarization fronts and associated auroral activities: 1. Conjugated observations and perspectives from global MHD simulation, *J. Geophys. Res.*, doi:10.1029/2012JA017676, in press.

Grigorenko, E. E., M. Hoshino, M. Hirai, T. Mukai, and L. M. Zelenyi (2009), "Geography" of ion acceleration in the magnetotail: X-line versus current sheet effects, *J. Geophys. Res.*, *114*, A03203, doi:10.1029/2008JA013811.

Harris, E. G. (1962), On a plasma sheath separating regions of oppositely directed magnetic field, *Nuovo Cimento*, *23*, 115–121.

Hoshino, M., T. Mukai, T. Yamamoto, and S. Kokubun (1998), Ion dynamics in magnetic reconnection: Comparison between numerical simulation and Geotail observations, *J. Geophys. Res.*, *103*, 4509–4530, doi:10.1029/97JA01785.

Hwang, K.-J., M. L. Goldstein, E. Lee, and J. S. Pickett (2011), Cluster observations of multiple dipolarization fronts, *J. Geophys. Res.*, *116*, A00I32, doi:10.1029/2010JA015742.

Li, S.-S., V. Angelopoulos, A. Runov, X.-Z. Zhou, J. P. McFadden, D. Larson, J. Bonnell, and U. Auster (2011), On the force balance around dipolarization fronts within bursty bulk flows, *J. Geophys. Res.*, *116*, A00I35, doi:10.1029/2010JA015884.

Lummerzheim, D., and M. Galand (2001), The profile of the hydrogen H_β emission line in proton aurora, *J. Geophys. Res.*, *106*, 23–32, doi:10.1029/2000JA002014.

McFadden, J. P., C. W. Carlson, D. Larson, M. Ludlam, R. Abiad, B. Elliott, P. Turin, M. Marckwordt, and V. Angelopoulos (2008), The THEMIS ESA plasma instrument and in-flight calibration, *Space Sci. Rev.*, *141*, 277–302, doi:10.1007/s11214-008-9440-2.

Nakamura, R., et al. (2002), Motion of the dipolarization front during a flow burst event observed by Cluster, *Geophys. Res. Lett.*, *29*(20), 1942, doi:10.1029/2002GL015763.

Ohtani, S., M. A. Shay, and T. Mukai (2004), Temporal structure of the fast convective flow in the plasma sheet: Comparison between observations and two-fluid simulations, *J. Geophys. Res.*, *109*, A03210, doi:10.1029/2003JA010002.

Onsager, T. G., M. F. Thomsen, R. C. Elphic, and J. T. Gosling (1991), Model of electron and ion distributions in the plasma sheet boundary layer, *J. Geophys. Res.*, *96*, 20,999–21,011, doi:10.1029/91JA01983.

Panov, E. V., et al. (2010), Multiple overshoot and rebound of a bursty bulk flow, *Geophys. Res. Lett.*, *37*, L08103, doi:10.1029/2009GL041971.

Runov, A., V. Angelopoulos, M. I. Sitnov, V. A. Sergeev, J. Bonnell, J. P. McFadden, D. Larson, K. Glassmeier, and U. Auster (2009), THEMIS observations of an earthward-propagating dipolarization front, *Geophys. Res. Lett.*, *36*, L14106, doi:10.1029/2009GL038980.

Runov, A., V. Angelopoulos, X.-Z. Zhou, X.-J. Zhang, S. Li, F. Plaschke, and J. Bonnell (2011a), A THEMIS multicase study of dipolarization fronts in the magnetotail plasma sheet, *J. Geophys. Res.*, *116*, A05216, doi:10.1029/2010JA016316.

Runov, A., et al. (2011b), Dipolarization fronts in the magnetotail plasma sheet, *Planet. Space Sci.*, *59*, 517–525, doi:10.1016/j.pss.2010.06.006.

Runov, A., V. Angelopoulos, and X.-Z. Zhou (2012), Multi-point observations of dipolarization front formation by magnetotail reconnection, *J. Geophys. Res.*, *117*, A05230, doi:10.1029/2011JA017361.

Schwartz, S. J., P. W. Daly, and A. N. Fazakerley (1998), Multi-spacecraft analysis of plasma kinetics, in *Analysis Methods for Multi Spacecraft Data*, edited by G. Paschmann and P. W. Daly, pp. 159–184, ESA, Bern.

Sergeev, V. A., R. C. Elphic, F. S. Mozer, A. Saint-Marc, and J. A. Sauvaud (1992), A two satellite study of nightside flux transfer events in the plasma sheet, *Planet. Space Sci.*, *40*, 1551–1572, doi:10.1016/0032-0633(92)90052-P.

Sergeev, V. A., V. Angelopoulos, S. Apatenkov, J. Bonnell, R. Ergun, R. Nakamura, J. P. McFadden, D. Larson, and A. Runov (2009), Kinetic structure of the sharp injection/dipolarization front in the flow-braking region, *Geophys. Res. Lett.*, *36*, L21105, doi:10.1029/2009GL040658.

Shabansky, V. P. (1971), Some processes in the magnetosphere, *Space Sci. Rev.*, *12*, 299–418.

Sibeck, D. G., and V. Angelopoulos (2008), THEMIS science objectives and mission phases, *Space Sci. Rev.*, *141*, 35–59, doi:10.1007/s11214-008-9393-5.

Sitnov, M. I., M. Swisdak, and A. V. Divin (2009), Dipolarization fronts as a signature of transient reconnection in the magnetotail, *J. Geophys. Res.*, *114*, A04202, doi:10.1029/2008JA013980.

Slavin, J. A., R. P. Lepping, J. Gjerloev, D. H. Fairfield, M. Hesse, C. J. Owen, M. B. Moldwin, T. Nagai, A. Ieda, and T. Mukai (2003), Geotail observations of magnetic flux ropes in the plasma sheet, *J. Geophys. Res.*, *108*(A1), 1015, doi:10.1029/2002JA009557.

Sonnerup, B. U. O. (1971), Adiabatic particle orbits in a magnetic null sheet, *J. Geophys. Res.*, *76*, 8211–8222.

Speiser, T. W. (1965), Particle trajectories in model current sheet: 1. Analytic solution, *J. Geophys. Res.*, *70*, 4219–4226.

Tsyganenko, N. A. (1995), Modeling the Earth's magnetospheric magnetic field confined within a realistic magnetopause, *J. Geophys. Res.*, *100*, 5599–5612, doi:10.1029/94JA03193.

Wu, P., and M. A. Shay (2012), Magnetotail dipolarization front and associated ion reflection: Particle-in-cell simulations, *Geophys. Res. Lett.*, *39*, L08107, doi:10.1029/2012GL051486.

Xing, X., L. R. Lyons, X.-Z. Zhou, V. Angelopoulos, E. Donovan, D. Larson, C. Carlson, and U. Auster (2012), On the formation of pre-onset azimuthal pressure gradient in the near-Earth plasma sheet, *J. Geophys. Res.*, *117*, A08224, doi:10.1029/2012JA017840.

Zelenyi, L. M., H. V. Malova, A. V. Artemyev, V. Y. Popov, and A. A. Petrukovich (2011), Thin current sheets in collisionless plasma: Equilibrium structure, plasma instabilities, and particle acceleration, *Plasma Phys. Rep.*, *37*, 118–160, doi:10.1134/S1063780X1102005X.

Zhang, X.-J., V. Angelopoulos, A. Runov, X.-Z. Zhou, J. Bonnell, J. P. McFadden, D. Larson, and U. Auster (2011), Current carriers near dipolarization fronts in the magnetotail: A THEMIS event study, *J. Geophys. Res.*, *116*, A00I20, doi:10.1029/2010JA015885.

Zhou, X.-Z., V. Angelopoulos, A. Runov, M. I. Sitnov, Q.-G. Zong, and Z. Y. Pu (2009), Ion distributions near the reconnection sites: Comparison between simulations and THEMIS observations, *J. Geophys. Res.*, *114*, A12211, doi:10.1029/2009JA014614.

Zhou, X.-Z., V. Angelopoulos, V. A. Sergeev, and A. Runov (2010), Accelerated ions ahead of Earthward-propagating dipolarization fronts, *J. Geophys. Res.*, *115*, A00I03, doi:10.1029/2010JA015481.

Zhou, X.-Z., V. Angelopoulos, V. A. Sergeev, and A. Runov (2011), On the nature of precursor flows upstream of advancing dipolarization fronts, *J. Geophys. Res.*, *116*, A03222, doi:10.1029/2010JA016165.

Zhou, X.-Z., V. Angelopoulos, A. Runov, J. Liu, and Y. S. Ge (2012), Emergence of the active magnetotail plasma sheet boundary from transient, localized ion acceleration, *J. Geophys. Res.*, doi:10.1029/2012JA018171, in press.